inactive as antisense inhibitors of gene expression. This inactivity is likely due to the low binding affinity and poor (unaided) cellular uptake of T-mC ODNs. Thus, our data questions many previous results describing antisense-mediated gene inhibition with T and C phosphorothioate and phosphodiester ODNs. The C-5 propyne–substituted phosphorothioates represent a new class of antisense ODNs that may prove to be universal reagents for the inhibition of gene expression.

REFERENCES AND NOTES

1. N. Bischofberger and R. W. Wagner, *Semin. Virol.* **3**, 57 (1992).
2. We have evaluated a variety of ODN analogs in a number of assay systems (*18*) and have found similar biological effects with antisense, mismatch, and scramble-sequence controls.
3. C. A. Stein, J. L. Tonkinson, L. Yakubov, *Pharmacol. Ther.* **52**, 365 (1991).
4. T. L. Fisher, T. Terhorst, X. Cao, R. W. Wagner, *Nucleic Acids Res.*, in press.
5. The TAg plasmid was derived from p5080 (*6*) in which the TAg-containing Kpn I–Bam HI fragment was cloned into pUC19 (Pharmacia, Piscataway, NJ); the β-gal plasmid was pRSVZ. The TAg and β-gal plasmids [needle concentrations of 0.006 and 0.16 μg/μl, respectively, in 80 mM KCl–50 mM Hepes (pH 7.3)] were nuclear microinjected into 100 CV-1 cells. Microinjection was performed on a microscope (Axiovert 10, Zeiss) with a pneumatic controller (PLI-188, Nikon, Garden City, NY) attached to a micromanipulator (MO-302, Narishige U.S.A., Greenvale, NY). The cells were subsequently incubated for 4.5 hours at 37°C, fixed, immunolabeled (*19*), and scored visually by fluorescence microscopy for TAg and β-gal expression. In the absence of co-injected ODNs, 95 ± 5% of the injected cells expressed β-gal and of these, 85 ± 5% co-expressed TAg.
6. L. C. Tack *et al.*, *J. Virol.* **63**, 3962 (1989).
7. M. Graessmann, G. Michaels, B. Berg, A. Graessmann, *Nucleic Acids Res.* **19**, 53 (1991).
8. B. C. Froehler, S. Wadwani, T. J. Terhorst, S. R. Gerrard, *Tetrahedron Lett.* **33**, 5307 (1992).
9. B. C. Froehler, R. J. Jones, X. Cao, T. J. Terhorst, *ibid.* **34**, 1003 (1993).
10. TAg-20a and TAg-20b containing 2′-deoxycytidine produced results identical to those observed with the T-mC ODNs.
11. The 15-nt ODN complementary to the TAg intron was 5′-UUUUCUAUUUUCAUG-3′.
12. A. M. Iribarren *et al.*, *Proc. Natl. Acad. Sci. U.S.A.* **87**, 7747 (1990).
13. Cells were incubated with ODNs for 24 hours, washed, and microinjected (100 cells per experiment) with the TAg and β-gal plasmids (*5*).
14. Cells were incubated with 5′-fluoresceinated TAg-15 (purified by polyacrylamide gel electrophoresis) for 2 hours in the presence of Texas Red–conjugated dextran (average molecular weight = 10,000; Molecular Probes, Eugene, OR; 1 mg/ml), a lysosomal marker. Fluorescence confocal microscopy of the live cells showed that >85% of the lysosomal vesicles contained both fluorophores.
15. M. Y. Chiang *et al.*, *J. Biol. Chem.* **266**, 18162 (1991).
16. TAg-15 or TAg-m10 (0.05 to 0.005 μM) was premixed with lipofectin (Gibco BRL, Gaithersburg, MD; 10 μM) and added to CV-1 cells in Opti-modified Eagle's medium (Gibco BRL). After 4 hours, the cells were washed and incubated for an additional 16 hours in Dulbecco's modified Eagle's medium plus 10% fetal bovine serum (FBS). One hundred cells were microinjected with the TAg and β-gal plasmids and analyzed (*5*).
17. The 20-nt ODN sequence used to target the 5′-untranslated region was 5′-GCCUCCUCACUACUUCUGGA-3′ and that used to target the translation initiation codon region was 5′-CAUCUUUGCAAAGCUUUUUG-3′. The T-mC phosphorothioate ODNs were each inactive at 1 μM, and each inhibited TAg and β-gal expression at 20 μM (*5*). The T-mC ODN targeted to the 5′-untranslated region specifically inhibited TAg expression at 5 μM, whereas the ODN targeted to the initiation codon partially inhibited both TAg and β-gal expression at 5 μM.
18. G. Anfossi, A. M. Gewirtz, B. Calabretta, *Proc. Natl. Acad. Sci. U.S.A.* **86**, 3379 (1989); A. Rosolen, L. Whitesell, N. Ikegaki, R. H. Kennett, L. Neckers, *Cancer Res.* **50**, 6316 (1990); M. Simons and R. D. Rosenberg, *Circ. Res.* **70**, 835 (1992); K. G. Draper, D. J. Ecker, C. K. Mirabelli, S. T. Crooke, International Patent Application WO 91/12811 (1991).
19. J. C. Hanvey *et al.*, *Science* **258**, 1481 (1992).
20. B. C. Froehler, in *Protocols for Oligonucleotides and Analogs: Synthesis and Properties*, S. Agrawal, Ed. (Humana, Totowa, NJ, 1993), pp. 63–80.
21. S. Young and R. W. Wagner, *Nucleic Acids Res.* **19**, 2463 (1991).
22. The control sequence was 5′-UUAUUAUCUUCUUCUUUUCU-3′ and contained 11 mismatches. Antisense ODNs were directly compared with control ODNs at concentrations tenfold more than the IC_{50} of the antisense ODN, and the control ODNs showed no activity.
23. M. Graessmann and A. Graessmann, *Methods Enzymol.* **101**, 482 (1983).

24. We thank T. Fisher, T. Terhorst, and S. Wadwani for technical assistance; J. Pipas for the p5080 plasmid; and J. Milligan for valuable discussions. All other cells and plasmids (pSV40 and pRSVZ) were purchased from the American Type Culture Collection. This work was supported in part by a contract from the Defense Advanced Research Projects Agency.

9 December 1992; accepted 23 March 1993

Relation of Phenotype Evolution of HIV-1 to Envelope V2 Configuration

Martijn Groenink,* Ron A. M. Fouchier, Silvia Broersen, Catriona H. Baker, Maarten Koot, Angélique B. van't Wout, Han G. Huisman, Frank Miedema, Matthijs Tersmette, Hanneke Schuitemaker

Biological variability of human immunodeficiency virus type–1 (HIV-1) is involved in the pathogenesis of acquired immunodeficiency syndrome (AIDS). Syncytium-inducing (SI) HIV-1 variants emerge in 50 percent of infected individuals during infection, preceding accelerated CD4$^+$ T cell loss and rapid progression to AIDS. The V1 to V2 and V3 region of the viral envelope glycoprotein gp120 contained the major determinants of SI capacity. The configuration of a hypervariable locus in the V2 domain appeared to be predictive for non-SI to SI phenotype conversion. Early prediction of HIV-1 phenotype evolution may be useful for clinical monitoring and treatment of asymptomatic infection.

There is increasing evidence for a role of biological variability of HIV-1 in the pathogenesis of AIDS (*1–4*). In the asymptomatic phase of infection, predominantly non–syncytium-inducing (NSI), monocytotropic HIV-1 variants can be detected (*5*). In about 50% of the cases SI HIV-1 variants emerge in the course of infection, preceding rapid CD4$^+$ T cell depletion and progression to AIDS (*6, 7*). Moreover, we recently obtained evidence that there is a major beneficial effect of zidovudine treatment in asymptomatic individuals who harbor NSI variants and do not develop SI variants during treatment (*8*). These findings prompted us to try to identify determinants within the viral genome that may be predictive for the future emergence of SI variants in an individual.

Previously we generated NSI and SI molecular HIV-1 clones from a single individual at the time of NSI to SI switch (*9*). In agreement with others, we have shown that the gene *env* is the major determinant responsible for differences in biological properties (*10–16*). Sequence analysis revealed that variation in the NH_2-terminal part of gp120, the C1 up to V4 region, segregated with the capacity to induce syncytia in peripheral blood mononuclear cells (PBMC) (*15*). To investigate if differences in SI capacity were determined by the C1 to V4 region, recombinant viruses were constructed in which sequences within this region were exchanged between an NSI and SI clone (Fig. 1).

Reciprocal exchanges between the NSI and SI clone of the V1 up to C2 region (Fig. 1, A and E), the COOH terminus of V1 ($V1_{C\text{-}term}$) up to the V2 region (Fig. 1, B and F), or the V3 up to V4 region (Fig. 1, C and G) resulted in recombinant viruses that induced occasional, small syncytia in PBMC. Primary SI isolates are characterized by their capacity to replicate and induce syncytia in the MT-2 T cell line (*17*). All recombinant viruses described above

Department of Clinical Viro-Immunology, Central Laboratory of the Netherlands Red Cross Blood Transfusion Service and Laboratory for Experimental and Clinical Immunology of the University of Amsterdam, Plesmanlaan 125, 1066 CX Amsterdam, The Netherlands.

*To whom correspondence should be addressed.

could productively infect MT-2 but, in contrast to the wild-type SI clone, induced only few and small syncytia in these cells. These findings indicated that both the $V1_{C\text{-}term}$ to V2 region as well as the V3 to V4 region independently contributed to SI capacity. Indeed, exchange of the complete V1 to V3 region between the NSI and SI clone fully conferred the wild-type phenotype (Fig. 1, D and H).

Previously, we demonstrated an association between SI capacity and the presence of positively charged amino acid (aa) residues at either one or both of aa positions 11 and 28 in V3 (*14*, *18*). To investigate if a V1 or V2 configuration (or both) exists that is associated with differences in SI capacity, sequence analysis was performed on a large panel of virus isolates obtained from participants of the Amsterdam cohort studies in whom the occurrence of a NSI to SI phenotype switch has been documented (*7*). All HIV-1 seropositive men in this cohort were clinically examined at least every 3 months, and PBMC were cryopreserved for virologic and immunological studies. Virus phenotype was determined by cocultivation of fresh patient PBMC with MT-2 cells (*7*, *17*). Virus isolates were obtained from individuals who never developed SI variants (stable NSI variants) or from individuals after the moment of NSI to SI conversion (switch NSI and SI variants) by coculture with PBMC.

The V1 domain appeared to be highly variable but did not reveal a clear-cut phenotype-associated sequence variation. The V2 domain appeared to be relatively conserved, particularly in aa residues 1 to 29 and 46 to 51 (Fig. 2). A hypervariable region within V2 was present between aa positions 29 to 46. Significant differences were observed in this hypervariable V2 locus among stable NSI variants, switch NSI variants, and SI variants. The mean length of the hypervariable V2 locus of switch NSI variants and SI variants was significantly increased as compared to stable NSI variants (Fig. 3). Within the hypervariable V2 locus, stable NSI variants contained a single, potential N-linked glycosylation site at aa position 33. In contrast, the hypervariable V2 locus in the majority of switch NSI and SI variants contained a potential N-linked glycosylation site (of the form N-X-T/S, where

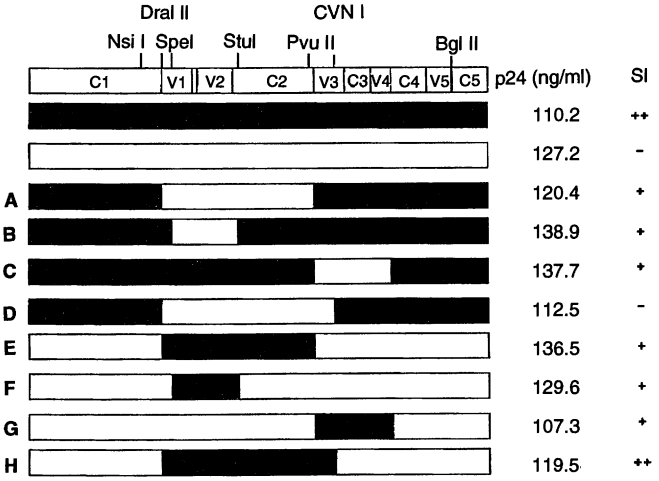

Fig. 1. SI capacity of the SI and NSI recombinant viruses. Closed bars indicate DNA sequences from the SI HIV-1 clone and open bars those from the NSI HIV-1 clone. SI clone 320.2A 1.2 and NSI clone 320.2A 2.1 (*15*) were used for the construction of recombinant viruses. Nsi I and Pvu II were used for exchanging V1 up to C2 (A and E), Spe I and Stu I for $V1_{C\text{-}term}$ up to V2 (B and F), Pvu II and Bgl II for V3 up to V4 (C and G), and Dra III and Cvn I for V1 up to V3 (D and H). In addition to V3 and V4, Pvu II and Bgl II also exchanged C4 and V5. However, the SI and NSI clone did not differ in these domains. Construction of recombinant proviruses, and evaluation of biological characteristics of the wild-type and recombinant proviruses, was as described (*15*). The wild-type and recombinant viruses did not differ in their peak virus production in PBMC, measured as p24 (*16*). To confirm SI capacity of the recombinant viruses, transmission of virus from PBMC to the MT-2 cell line was attempted by both cocultivation and cell free transmission (*17*). Differences in SI capacity of wild-type and recombinant viruses were similar in both PBMC and MT-2. All transfection and transmission studies were performed at least three times, with identical results. PCR and sequence analysis demonstrated that the nucleotide sequence of the C1 up to V4 region of the recombinant viruses was not altered by replication in PBMC or the MT-2 T cell line over the time course of the experiments (*19*). ++: wild-type SI capacity, which resulted in death of the MT-2 culture 7 to 10 days after infection; +: induction of only few and small syncytia, which did not cause death of the MT-2 culture; −: no syncytia observed in PBMC and not transmissible to the MT-2 cell line.

Fig. 2. Alignment of V2 sequences with the consensus sequence of the analyzed variants. Similarity is shown as dashes, gaps as dots. Nested PCR and sequence analysis of V1–V2 was performed as described (*14*). Primers are as described (*23*). Abbreviations for the amino acid residues are: A, Ala; C, Cys; D, Asp; E, Glu; F, Phe; G, Gly; H, His; I, Ile; K, Lys; L, Leu; M, Met; N, Asn; P, Pro; Q, Gln; R, Arg; S, Ser; T, Thr; V, Val; W, Trp; and Y, Tyr.

HIV Isolate	1 10 20 30 40 51 CSFNITTSIRDKVQKEYALFYKLDVVPID.NDNTS.....YRLISC
SI Variants	
Ams-161.15	-------N-------T-------------.-----HNDNTSYRS.------
ACH-320.2A.1.1	----------------------NS------D.--ATT.KNKTTR.NFK--H-
Ams-16.2	-------A-----RR-HT----------.--....KKNIT..S.----H-
ACH-39.14.2	-------N-------V--T------I----D.E.-N..KNNTNYTN------
Ams-72.3.2	-------L---M----------------.K--D....NTS.....------
ACH-224.25.5	--------TGE---.DF-Y------A--...-.----....T..R..-----
ACH-571.16.2	----------M----------------.-AKD....NTS.....------
Ams-169.2	-------NR---M---Q---------I--N.-RDN-G..NTSYSS.F---H-
ACH-479.5	----------------------R--------.--KDN..KNNS.R..-----
ACH-168.7	----------------------H----L-.......KNNT...N------
Ams-55	----V--LV---MK--H-----R-------..KE-ND...NTS.....----N-
ACH-704.2	-------DM--RIERV---------E---.--T-.....------------
ACH-373.38	----------R----------------.-E-.....------------
Ams-32	-------R-------------P-I-----.-T-NT..K.T....N------
Ams-127.4.2	-------GM---I--V---L---------.-N-NTT......R..------
Switch NSI Variants	
Ams-161.42	-------N-------T-------------D.-.ND...NTS....---T--
ACH-320.2A.2.1	---K---NMK--A-I--------------.-.-NT...NTSYTS.------
Ams-16.3	-------V------.R-------------N.-----....NTS.....----
ACH-39.14.4	-------N---M--V--T------I----DKT-NT...NYT...N------
Ams-72.2.1	---R-S-N-K---M---------------D-.--T...N.S.....------
ACH-224.23.2	--------TGE----.D--Y-------E---..-.I-....T..R..-----
ACH-571.16.6	-------N----M----------------.-AKD....NTS.....-----
Ams-169.14	-T------N----M----------------..K.-E..NTSYSS.-----N-
Stable NSI Variants	
ACH-239.11	----V----E--RK----------I----.-----.....-T--N-
Ams-44	----------R----------------.-----.....----M--
Ams-168.2	-----N---------K----------------.-N-R-.....-----N-
Ams-96.1	----------I--GH-V-D---I-----.-.-STS.....------
ACH-424	-------N----M----------------.-E---.....------
Ams-24	----------IK----------------.-----.....R..------
ACH-15.9	----------------T--N--------.T-----.....-K----
ACH-172.1	-------SM-----K----------------.-G-NT....T..K..-----
ACH-525	-------N----------F----------.---D-....T...S.------
ACH-638	----------RI.-RIS--NS------K.---S-.....F---N-
Ams-179	----------K-----L-----I-----.---HT.....------
Ams-180	----------M----------I---N.SG---Y.....---T--
Ams-181	-------R----------------...--T..K.....----N-
Ams-182	----------N-------R-FI----I--.-.---.....------

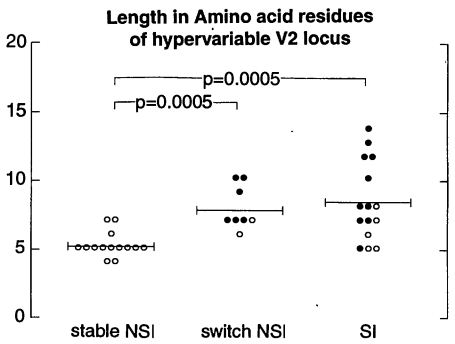

Fig. 3. Comparison of the length of the hypervariable V2 locus and the presence of potential N-linked glycosylation sites in stable NSI HIV-1 variants, switch NSI HIV-1 variants, and SI HIV-1 variants. Bars indicate means. The Mann-Whitney U test was used to determine statistical significance of differences on the basis of length of the hypervariable V2 locus. Open circles represent viruses that lacked a potential N-linked glycosylation site at aa position 39, closed circles represent viruses in which a potential N-linked glycosylation site at aa position 39 was present.

N is Asn, X is variable, S is Ser, and T is Thr) at aa position 39 (Fig. 3 and Table 1) instead of or in addition to the potential N-linked glycosylation site at aa position 33. Although switch NSI and SI variants did not significantly differ in length and position of the potential N-linked glycosylation site, the hypervariable V2 locus of SI variants contained significantly more positively charged aa residues than stable NSI and switch NSI variants (Fig. 2, stable NSI versus SI $P = 0.0026$ and switch NSI versus SI $P = 0.0306$ according to the Mann-Whitney U test). In accordance with our previous observations (*14*), none of the NSI variants, but all SI variants, exhibited a positively charged aa residue at either position 11 or 28 of V3 (*19*).

To determine the time at which switch NSI variants, as defined by the configuration of the hypervariable V2 locus, were present relative to the emergence of SI variants, clonal HIV-1 isolates were obtained from four individuals 18 to 36 months before the phenotype switch (Fig. 4). V2 sequence analysis revealed that, at least 36 months before SI variants emerged, switch NSI variants were detectable.

We next investigated whether individuals who develop AIDS in the absence of SI variants, harbored stable NSI variants exclusively. All 55 biological clonal HIV-1 isolates obtained from an individual (ACH-424 in Fig. 2) over a 4-year period, from 1 month after seroconversion up to 1 year after AIDS diagnosis, had the stable V2 NSI configuration (*19*).

In this study we demonstrated that the $V1_{C\text{-term}}$ to V2 and V3 domain, identified before to be involved in macrophage tropism (*10–12*), are together the main determinants of SI capacity of HIV-1. This suggests that variation in V2 and V3 influences the virus-cell fusion events either by inducing changes in gp120 conformation after binding to CD4, or by affecting the interaction of gp120 with cell type–specific accessory molecules as has also been suggested by studies with monoclonal antibodies directed against V2 and V3 (*20–22*).

We describe distinct V2 configurations for NSI variants that do or do not have the capacity to give rise to SI variants. Since viruses with a switch V2 configuration were present, in some cases at least 3 years before phenotype conversion it is tempting to speculate that these biologically distinct viruses represent true strains of HIV-1 present at the time of infection. However, data thus far are in favor of the hypothesis that switch NSI variants are derived from NSI viruses shortly after seroconversion.

Although the hypervariable V2 locus of switch NSI variants and SI variants did not differ in length and location of potential N-linked glycosylation site, they differed significantly in the number of positively charged amino acid residues. Thus, SI viruses have gone through additional changes in V2 that may be necessary for the appearance of the subsequent changes in V3; it is the combination of changes in V2 and V3 that give the SI phenotype. Our exchange studies and more recent results by others (*24*) support this concept. On the basis of the configuration of the hypervariable V2 locus, the NSI clone had a switch NSI phenotype (ACH-320.2A.2.1 in Fig. 2). Substitution of the region from V3 to V4 of the switch NSI clone with the corresponding region of the SI clone, conferred only an intermediate SI phenotype on the switch NSI clone. Moreover, exchange studies between a clone that met our criteria of the stable NSI phenotype and an SI clone identified the same region as being responsible for differences in biological phenotype (*11*). Together, these data support the idea of functional involvement of V2 in SI capacity, independent of viral background. However, additional studies of the mechanism involved are required.

The identified hypervariable V2 locus allows for an early discrimination between stable NSI variants and NSI variants with the potential to convert to the SI phenotype. This opens up the potential for diagnostics based on the polymerase chain reaction (PCR). Given the influence of HIV-1 phenotype on AIDS pathogenesis (*7*) and the phenotype-dependent efficacy of zidovudine treatment (*8*), the ability to predict HIV-1 phenotype evolution may be useful for clinical monitoring and for optimal therapeutic intervention in asymptomatic HIV-1 infection.

Table 1. Comparison of potential N-linked glycosylation sites (N-*X*-S/T). The probability of a random distribution as measured by the Fisher exact test was as follows. Potential glycosylation site only at position 33: stable NSI versus switch NSI, $P = 0.0023$; stable NSI versus SI, $P = 0.0004$. Potential glycosylation site only at position 39: stable NSI versus switch NSI, $P = 0.0096$; stable NSI versus SI, $P = 0.0015$.

Variant	*n*	Potential N-*X*-S/T at position		
		33	33 and 39	39
Stable NSI	14	13	0	0
Switch NSI	8	2	2	4
SI	15	4	2	8

HIV-1 Isolate	Month after SC	Pheno-type	1 10 20 30 40 51 CSFNITTSIRDKVQKEYALFYKLDVVPID.NDNTS.....YRLISC	No. of Clones
Ams-72.1	41	NSI	--------L---M----------.-----.....------	3
	41	NSI	--------L---M----------.-TID....NTS....------	3
Ams-72.2	71	NSI	---R-S-N-K--M----------D-.--T...N.S....------	1
Ams-72.3	71	SI	--------L---M----------.K--D....NTS....------	12
ACH-224.18	27	NSI	--------TGE---.D--Y------E--E...-G-...NGSTR..------	1
ACH-224.23	42	NSI	--------TGE---.D--Y------E--..-.-I-....T..R..------	4
ACH-224.25	48+	SI	--------TGE---.DF-Y------A--..-.---....T..R..------	1
ACH-571.12	12	NSI	-------N----M----------.-----.....------	2
	12	NSI	-------N----M----------.---D....NTS....------	1
ACH-571.16	30+	NSI	-------N----M----------.-AKD....NTS....------	1
ACH-571.16	30	SI	----------M----------.-AKD....NTS....------	3
Ams-169*	3	NSI	-T-----N----M----------L-.SS-NT.....R----N-	1
	3	NSI	-T-----N----M----------..K..-E..NTSYSS.----N-	5
Ams-169.14	39+	NSI	-T-----N----M----------..K..-E..NTSYSS.----N-	1
Ams-169.2	39	SI	-------NR---M---Q--------I--N.-RDN-G..NTSYSS.F---H-	2

Fig. 4. V2 sequences of biological clonal HIV-1 variants (Ams-72, ACH-224, ACH-571, and Ams-169) obtained from PBMC samples of four individuals before and at the NSI to SI phenotype switch. The V2 sequences are aligned with the consensus sequence as shown in Fig. 2. *, Moment of seroconversion of 169 is unknown. The early Ams-169 was obtained 3 months after intake in the study; +, estimated moment of NSI to SI phenotype switch.

REFERENCES AND NOTES

1. B. Asjo *et al.*, *Lancet* ii, 660 (1986).
2. C. Cheng-Mayer, D. Seto, M. Tateno, J. A. Levy, *Science* **240**, 80 (1988).
3. M. Tersmette *et al.*, *J. Virol.* **63**, 2118 (1989).
4. R. I. Connor, H. Mohri, Y. Cao, D. D. Ho, *ibid.* **67**, 1772 (1993).
5. H. Schuitemaker *et al.*, *J. Virol.* **66**, 1354 (1992).
6. M. Tersmette *et al.*, *Lancet* **335**, 983 (1989).
7. M. Koot *et al.*, *Ann. Int. Med.* **118**, 681 (1993).
8. M. Koot *et al.*, *J. Infect. Dis.*, in press.
9. M. Groenink *et al.*, *J. Virol.* **65**, 1968 (1991).
10. P. Westervelt *et al.*, *ibid.* **66**, 2577 (1992).
11. T. Shioda, J. A. Levy, C. Cheng-Mayer, *Nature* **349**, 167 (1991).
12. W. A. O'Brien *et al.*, *ibid.* **348**, 69 (1990).
13. S. S. Hwang, T. J. Boyle, H. K. Lyerly, B. R. Cullen, *Science* **253**, 71 (1991).
14. R. A. M. Fouchier *et al.*, *J. Virol.* **66**, 3183 (1992).
15. M. Groenink *et al.*, *ibid.*, p. 6175.
16. M. Tersmette *et al.*, *Virology* **171**, 149 (1989).
17. M. Koot *et al.*, *AIDS* **6**, 49 (1992).
18. J. J. De Jong *et al.*, *J. Virol.* **66**, 757 (1992).
19. M. Groenink *et al.*, unpublished data.
20. D. D. Ho *et al.*, *Proc. Natl. Acad. Sci. U.S.A.* **88**, 8949 (1991).
21. M. S. C. Fung *et al.*, *J. Virol.* **66**, 848 (1992).
22. Q. J. Sattentau and J. P. Moore, *J. Exp. Med.* **174**, 407 (1991).
23. The V1–V2 primers are given with their positions in the HIV-1 clone HXB2 (+, sense; −, antisense): primer 1, GCCTGTGTACCCACAGACCCCAA (+, 6463); primer 2, GAGGATATAATCAGTTTATGGGAT (+, 6562); primer 3, TTCAAATGATACCTTTGGACAGGC (−, 6956); and primer 4, CCTAATTCCATGTGTACATTGTAC (−, 6833). V1–V2 was amplified with primer 1 and 4 in the first reaction and 2 and 3 in the second reaction. The V1 to V2 primers were based on the consensus of the

sequences published by G. Myers, A. B. Rabson, J. A. Berzofsky, T. F. Smith, F. Wong-Staal, *Human retroviruses and AIDS. A compilation and analysis of nucleic acid and amino acid sequences* (Theoretical Biology and Biophysics, Los Alamos, 1990).
24. A. C. Andeweg, P. Leeflang, A. D. M. E. Osterhaus, M. L. Bosch, *J. Virol.*, in press.
25. The authors wish to thank R. E. Y. de Goede, R. C. M. van der Jagt, and N. A. Kootstra for technical assistance as well as R. A. W. van Lier and L. Meyaard for critical reading of the manuscript. Supported in part by grant 900-502-104 from the Netherlands Organization for Scientific Research and by grants 92-025, 92-024, and 90-016 from RGO/WVC (Ministry of Public Health). This work was performed as part of the Amsterdam Cohort studies on AIDS.

23 April 1993; accepted 10 May 1993

Neuroprotective Effects of Glutamate Antagonists and Extracellular Acidity

David A. Kaku, Rona G. Giffard, Dennis W. Choi*

Glutamate antagonists protect neurons from hypoxic injury both in vivo and in vitro, but in vitro studies have not been done under the acidic conditions typical of hypoxia-ischemia in vivo. Consistent with glutamate receptor antagonism, extracellular acidity reduced neuronal death in murine cortical cultures that were deprived of oxygen and glucose. Under these acid conditions, *N*-methyl-D-aspartate and α-amino-3-hydroxy-5-methyl-4-isoxazolepropionate–kainate antagonists further reduced neuronal death, such that some neurons tolerated prolonged oxygen and glucose deprivation almost as well as did astrocytes. Neuroprotection induced by this combination exceeded that induced by glutamate antagonists alone, suggesting that extracellular acidity has beneficial effects beyond the attenuation of ionotropic glutamate receptor activation.

Glutamate receptor antagonists reduce the neuronal death induced by hypoxia-ischemia in vivo, most likely by reducing excitotoxic injury (*1*). Glutamate antagonists also reduce neuronal death in vitro after hypoxic insults (*2*). However, most in vitro studies have been performed at physiological extracellular pH (7.2 to 7.4), whereas the pH of hypoxic-ischemic brain in vivo is usually more acidic (pH 6.4 to 6.9).

Extracellular acidity itself may contribute to brain injury (*3*), perhaps by damaging astrocytes and promoting tissue necrosis (*4*), but it may also improve neuronal survival by reducing excitotoxicity (*5–8*). Glutamate receptor–mediated whole cell currents in hippocampal neurons, especially currents mediated by *N*-methyl-D-aspartate (NMDA) receptors, are attenuated at acidic extracellular pH (pH 6.6) (*5*). Cortical (*6*) and cerebellar neurons (*7*) are similarly affected, and moderate acidity reduces rapidly triggered glutamate neurotoxicity and hypoxic neuronal injury in cell cultures and hippocampal slices (*6, 8*).

We examined the neuroprotective efficacy of glutamate antagonists in vitro, under conditions of extracellular acidity relevant to hypoxia-ischemia in vivo (*9*). Loss of parenchymal neuroprotective efficacy might occur if such acidity eliminated the contribution of glutamate receptors to excitotoxic injury. In that case, neuroprotective effects documented in vivo might be explained by other actions, for example, effects on blood flow (*10*).

Mixed neuronal and glial cell cultures, and astrocyte cell cultures, derived from fetal mice on days 15 through 17 of embryonic development were cultured for 14 to 16 days (*11*). We deprived neuronal-glial cultures of oxygen and glucose by exchanging the bathing medium within a hypoxia chamber (<0.3% O_2) (*12*).

Oxygen and glucose deprivation at pH 7.4 for longer than 40 min induced gross neuronal degeneration within 24 hours, associated with lactate dehydrogenase (LDH) efflux into the bathing medium (*13*). The glial layer remained morphologically intact and excluded trypan blue dye.

Table 1. Enhancement of neuroprotection by MK-801 in the presence of extracellular acidity. Sister cultures were deprived of oxygen and glucose for 120 min, alone (CTRL) or in the presence of 10 μM MK-801 or 10 μM CNQX, at pH 7.4 or 6.4. Values represent the mean LDH ± SEM (n = 4), measured 24 hours after exposure, scaled to the mean LDH found in control injury at pH 7.4 (= 100). Significant difference ($P < 0.05$) from control injury, pH 7.4 (*), or from control injury, pH 6.4 (†), was determined by analysis of variance and Student-Neuman-Keuls' test.

System	LDH	Significance
	pH = 7.4	
CTRL	100 ± 11	
10 μM MK-801	61 ± 5	*
	pH = 6.4	
CTRL	63 ± 2	*
10 μM MK-801	9 ± 4	*†
10 μM CNQX	41 ± 9	*

Complete neuronal degeneration was induced by oxygen-glucose deprivation for 70 to 100 min (Fig. 1). In astrocyte cultures, glial damage and LDH efflux did not occur until deprivation approached 5 hours. Lowering the pH of the medium to 6.4 markedly attenuated the neuronal death induced by deprivation for 40 to 80 min; however, this protective effect diminished with deprivation for longer periods and was largely absent after deprivation for 100 min (Fig. 1).

We examined the effect of glutamate receptor antagonists at pH 6.4, using periods of oxygen-glucose deprivation sufficient to override the protective effect of acidity alone. We found that the noncompetitive NMDA antagonist MK-801 (*14*) reduced neuronal injury (Table 1 and Fig. 2), whereas the α-amino-3-hydroxy-5-methyl-4-isoxazoleproprionate (AMPA)–kainate receptor antagonist 6-cyano-7-nitro-quinoxaline-2,3-dione (CNQX) (*15*) alone did not have a significant neuroprotective effect (Table 1). The noncompetitive NMDA antagonist dextrorphan (*16*) and the competitive NMDA antagonist CGS-19755

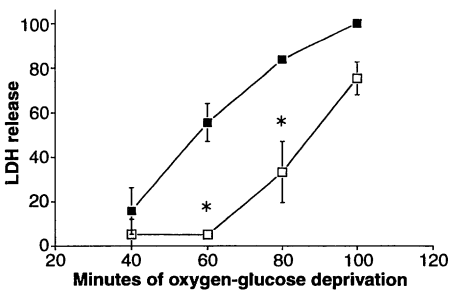

Fig. 1. Extracellular acidity reduces neuronal injury induced by oxygen-glucose deprivation. Sister cultures (derived from the same plating) were exposed to medium lacking oxygen and glucose for the periods indicated, at pH 7.4 (filled squares) or pH 6.4 (open squares). Values represent the mean LDH ± SEM (n = 4), scaled to the near complete neuronal degeneration (assessed by phase-contrast microscopy and trypan blue staining) induced by 100 min of oxygen-glucose deprivation at pH 7.4 (= 100). An asterisk indicates a significant difference from the same duration of deprivation at pH 7.4 ($P < 0.05$) by analysis of variance and Student-Neuman-Keuls' test. Points without error bars indicate SEM less than the width of the plotted point, and background LDH measured in cultures exposed to sham wash has been subtracted from all values.

D. A. Kaku, Department of Neurology and Neurological Sciences, Stanford University School of Medicine, Stanford, CA 94305.
R. G. Giffard, Department of Anesthesia, Stanford University School of Medicine, Stanford, CA 94305.
D. W. Choi, Department of Neurology, Washington University School of Medicine, St. Louis, MO 63110.
*To whom correspondence should be addressed.